PHOTOSYNTHETICA
International Journal for Photosynthesis Research

DOI 10.32615/ps.2022.040 PHOTOSYNTHETICA 60 (3): 457-464, 2022

Diurnal decline in the photosynthetic capacity of uppermost leaves in an eggplant canopy grown in a horticultural greenhouse

K. NOMURA*,+, M. SAITO*, M. ITO*, S. YAMANE**, T. IWAO*, I. TADA*, T. YAMAZAKI*, S. ONO***, D. YASUTAKE*,#, and M. KITANO*

*IoP Collaborative Creation Center, Kochi University, 200 Otsu, Monobe, Nankoku City, 783-8502 Kochi, Japan**
*Faculty of Agriculture and Marine Sciences, Kochi University, 200 Otsu, Monobe, Nankoku City, 783-8502 Kochi, Japan***
*Bioenvironmental Sciences, Kyushu University, 744 Motooka, Nishi-ku, Fukuoka City, 819-0395 Fukuoka, Japan****
Faculty of Agriculture, Kyushu University, 744 Motooka, Nishi-ku, Fukuoka City, 819-0395 Fukuoka, Japan#

Abstract

Parameters representing leaf photosynthetic capacity, namely, the maximal carboxylation rate (V_{cmax}), maximal electron transport rate (J_{max}), and triose phosphate-utilization rate (T_p), can vary depending on various factors. The present study investigated diurnal variations in V_{cmax}, J_{max}, and T_p of uppermost leaves of soil-grown, well-watered eggplant in a greenhouse based on the simultaneous measurements of leaf gas exchange and chlorophyll fluorescence. The values of net photosynthetic rates and electron transport rates plotted against intercellular CO_2 concentrations were noticeably higher in the morning than in the afternoon. Significant differences were detected among the values of V_{cmax}, J_{max}, and T_p obtained at different times of day (08:30, 11:00, 13:30, and 16:00 h). All three parameters tended to decline as the time of day advanced; compared to the values at 08:30 h, V_{cmax}, J_{max}, and T_p declined by approximately 15% at 16:00 h. Among the three parameters, T_p appeared to be the most sensitive to time.

Keywords: CO_2–photosynthesis curve; diurnal variation; Farquhar–von Caemmerer–Berry photosynthesis model; horticultural crop; photosynthesis limitation; triose phosphate utilization.

Introduction

Photosynthesis is the primary process of fixing atmospheric CO_2 and has been a focus of interdisciplinary studies due to its importance in, *e.g.*, food production (Murchie and Lawson 2013), bioenergy production (Larkum 2010), and climate change (Piao *et al.* 2013). In modern horticultural crop production, in which environmental conditions in greenhouses can be artificially modified, the improvement of crop photosynthesis *via* environmental controls is regarded as a key to increasing crop growth and yields (Prior *et al.* 2011).

Net photosynthetic rates (gross photosynthetic rate minus respiration) can be estimated by several methods.

Highlights

- Diurnal variations in eggplant leaf photosynthetic capacity were investigated
- Concurrent measurements of gas exchange and chlorophyll fluorescence were conducted
- V_{cmax}, J_{max}, and TPU declined by approximately 15% toward the end of the day

Received 11 June 2022
Accepted 10 August 2022

+Corresponding author
e-mail: jm-koichi.nomura@kochi-u.ac.jp

Acknowledgments: This study was supported by a Cabinet Office grant-in-aid, the Advanced Next-Generation Greenhouse Horticulture by IoP (Internet of Plants), Japan, and JSPS KAKENHI grant numbers JP21K14946 and JP22H02468. The authors thank Nana Miyatake and Chiyuki Yamanaka for assisting with the measurements.
Conflict of interest: The authors declare that they have no conflict of interest.

The most direct method is to employ a measurement system (*e.g.*, the chamber method and eddy covariance method) that monitors changes in atmospheric CO_2 concentrations caused by photosynthesis (Baldocchi 2003, Long and Bernacchi 2003). These direct measurements, however, require special equipment and expertise and thus have limited scalability in both time and space. Thus, rather than direct measurements, photosynthetic rates are often estimated using mathematical models based on easily measurable environmental elements, such as solar radiation, atmospheric CO_2 concentration, air temperature, humidity, and wind velocity (Kimura *et al*. 2020). In this way, net photosynthetic rates have been estimated at various scales from single leaves to the globe (Ryu *et al*. 2019).

Among the mathematical models used for estimating net photosynthetic rates, the model proposed by Farquhar, von Caemmerer, and Berry (hereafter called the FvCB model, Farquhar *et al*. 1980) and later extended by Sharkey (1985) provides a robust mechanistic representation of single-leaf net photosynthetic rates of C_3 plants and has been used in many modeling studies (Rogers *et al*. 2017). The FvCB model can be combined with other models of stomatal conductance (Ball *et al*. 1987, Medlyn *et al*. 2011) and the transport of mass and energy between the leaf and the surrounding environment (Gaastra 1959, Jones 2013). This model combination enables the estimation of the single-leaf net photosynthetic rate from environmental elements (Collatz *et al*. 1991). Additionally, the FvCB model can be scaled up to estimate plant canopy photosynthetic rates by considering the amount of leaves (*i.e.*, leaf area index), radiation transfer inside the canopy, and the vertical distribution of the photosynthetic capacity of leaves (De Pury and Farquhar 1997, Nomura *et al*. 2021).

To use the FvCB model for estimating net photosynthetic rates from environmental elements, several model parameters should be assigned *a priori*. Among these model parameters, the maximal carboxylation rate (V_{cmax}), maximal electron transport rate (J_{max}), and triose phosphate-utilization rate (T_p) represent the photosynthetic capacity of a single leaf and can influence the model estimation of photosynthetic rates. Values of V_{cmax}, J_{max}, and T_p differ widely depending on plant functional traits (Walker *et al*. 2017) and can acclimate to environmental conditions such as light (Parelle *et al*. 2006), temperature (Yamori *et al.* 2014), and CO_2 concentration (Leakey *et al.* 2009). Among the factors potentially influencing V_{cmax}, J_{max}, and T_p, the effect of time of day has been relatively less studied (Singsaas *et al*. 2000, Kets *et al*. 2010, Nascimento and Marenco 2013, Fabre *et al*. 2019, Stinziano *et al*. 2020). A typical response of V_{cmax}, J_{max}, and T_p to time is a decline toward the end of the day (Tanizaki *et al.* 2022). Mechanisms of this decline are not fully understood but are suggested to be involved in the feedback inhibition of photosynthesis due to accumulated carbon (Fabre *et al.* 2019) and diurnal decline in mesophyll conductance (Flexas *et al*. 2013) due to changes in leaf hydraulic conductance (Brodribb and Holbrook 2004) and the movement of chloroplasts (Tholen *et al*. 2008, Maai *et al*. 2020). The extent of the decline in V_{cmax}, J_{max}, and T_p in the literature differs widely among species (Stinziano *et al*. 2020) but has not yet been investigated in horticultural crops.

The objective of the present study was to investigate diurnal variations in the V_{cmax}, J_{max}, and T_p of uppermost leaves of soil-grown, well-watered eggplant (*Solanum melongena* L.) in a greenhouse based on simultaneous measurements of leaf gas exchange and chlorophyll fluorescence. The single-leaf photosynthetic rate (P_N) and electron transport rates (J_F), from which V_{cmax}, J_{max}, and T_p were estimated, were measured under varying CO_2 concentrations. Two different experiments were conducted; in the first experiment, leaf gas-exchange measurements were repeated on the same leaves at four different times of day (08:30, 11:00, 13:30, and 16:00 h). In the second experiment, leaves were randomly selected at each of the four diurnal measurements at 08:30, 11:00, 13:30, and 16:00 h.

Materials and methods

Plant material: The eggplant was cultivated in a greenhouse (ground area = 7.5 × 20 m^2, height = 3.0 m) covered with a diffuse ethylene tetrafluoroethylene (ETFE) film located on the Monobe Campus of Kochi University (33°33'4"N, 133°40'37"E). In the greenhouse, seedlings of eggplants (the 'Ryoma' variety grafted onto rootstocks of 'Daitaro') were transplanted onto four rows of ridges on 3 September 2021, with a planting density of 1.5 plants m^{-2} (135 cm between rows and 50 cm between plants within a row). Each ridge was provided with two parallel drip irrigation tubes and covered with white plastic mulch. The amount of irrigation water was adjusted depending on the solar radiation and leaf area. Together with irrigation water, liquid fertilizer (N:P:K =

Abbreviations: *ANOVA* – analysis of covariance; $C_{a,house}$ – CO_2 concentration inside the greenhouse; C_i – CO_2 concentration in the intercellular space of the leaf; F_m' – light-adapted maximum fluorescence yield; F_s – steady-state fluorescence yield; I – incident PPFD on the leaf; I_2 – usable PPFD absorbed by photosystem II; J – electron transport rate; J_F – electron transport rate estimated from chlorophyll fluorescence; K_c – Michaelis–Menten constants of Rubisco for carboxylation; K_o – Michaelis–Menten constants of Rubisco oxygenation; O – O_2 concentration in the intercellular space of the leaf (210 mmol mol^{-1}); P_c – net photosynthetic rate limited by Rubisco; P_j – net photosynthetic rate limited by the regeneration of RuBP; P_N – net photosynthetic rate; P_p – net photosynthetic rate limited by the use of triose phosphate; R_d – mitochondrial respiration rate; RH – relative humidity; RH_{house} – relative humidity inside the greenhouse; S_{out} – outside solar radiation; $T_{a,house}$ – air temperature inside the greenhouse; T_L – leaf temperature; T_p – triose phosphate-utilization rate; TPU – triose phosphate utilization; V_{cmax} – maximal carboxylation rate; α – fraction of glycolate carbon not returned to the chloroplast; α_L – absorptance of leaves; β_{PSII} – fraction of absorbed PPFD that reaches photosystem II; Γ^* – CO_2-compensation point without R_d; θ – empirical curvature factor; Φ_{max} – maximum quantum yield of photosystem II; Φ_{PSII} – quantum yield of photosystem II.

15:15:15, *Yoeki Doko No. 3*, *OAT Agrio Co.*, *Ltd.*, Tokyo, Japan; diluted 2,000 times) was provided. A base fertilizer was provided before transplantation [N:P:K = 7:8:5; *Amino ace*, *Cosmo Suisan*, Tottori, Japan; amounting to 22 g(N) m^{-2}]. The top greenhouse windows were opened during the daytime depending on the greenhouse temperature. During the winter, a heater was operated to maintain greenhouse nighttime temperatures above 12°C. The daytime CO_2 concentration was maintained above 400 ppm using a CO_2 generator. The plants were pruned to two shoots, which were trained with strings tied to two parallel wires located 1.8 m above the ground. The tops of the two shoots were pruned around the first week of December 2021, when the plants reached the height of the wire. On each node, a fruit-leaf unit containing one fruit and three leaves was maintained.

Photosynthesis model: Photosynthetic parameters were estimated based on the FvCB single-leaf C_3 photosynthesis model (Farquhar *et al.* 1980) extended by Sharkey (1985). This model assumes that the photosynthetic rate of a single leaf is limited by the slower of three processes: the carboxylation of ribulose-1,5-bisphosphate (RuBP) by ribulose bisphosphate carboxylase-oxygenase (Rubisco), the regeneration of RuBP, and the utilization of triose phosphate:

$$P_N = \min(P_c, P_j, P_p) \tag{1}$$

where P_N is the single-leaf net photosynthetic rate, P_c is the net photosynthetic rate limited by Rubisco, P_j is the net photosynthetic rate limited by the regeneration of RuBP, and P_p is the net photosynthetic rate limited by the use of triose phosphate. P_c, P_j, and P_p are given by von Caemmerer (2000):

$$P_c = \frac{V_{cmax}(C_i - \Gamma^*)}{C_i + K_c(1 + O/K_o)} - R_d \tag{2}$$

$$P_j = \frac{J(C_i - \Gamma^*)}{4C_i + 8\Gamma^*} - R_d \tag{3}$$

$$P_p = \frac{(C_i - \Gamma^*)(3T_p)}{[C_i - (1 + 3\alpha/2)\Gamma^*]} - R_d \tag{4}$$

where V_{cmax} is the maximal carboxylation rate, J is the electron transport rate, T_p is the triose phosphate-utilization rate, R_d is the mitochondrial respiration rate, C_i is the CO_2 concentration in the intercellular space of the leaf, Γ^* is the CO_2-compensation point without R_d, K_c and K_o are the Michaelis–Menten constants of Rubisco for carboxylation and oxygenation, respectively, O is the O_2 concentration in the intercellular space of the leaf (210 mmol mol^{-1}), and α is the fraction of glycolate carbon not returned to the chloroplast. In Eq. 3, J is expressed as a nonrectangular hyperbola:

$$J = \frac{I_2 + J_{max} - \sqrt{(I_2 + J_{max})^2 - 4\theta I_2 J_{max}}}{2\theta} \tag{5}$$

where J_{max} is the maximal electron transport rate, θ is an empirical curvature factor, and I_2 is the usable photosynthetic photon flux density (PPFD) absorbed by PSII, expressed as:

$$I_2 = I\alpha_L\beta_{PSII}\Phi_{max} \tag{6}$$

where I is the PPFD incident on the leaf, α_L is the absorptance of leaves, β_{PSII} is the fraction of absorbed PPFD that reaches PSII, and Φ_{max} is the maximum quantum yield of PSII (von Caemmerer 2000, Bernacchi *et al.* 2003).

Measurement of single-leaf photosynthesis: Diurnal variations in three photosynthetic parameters (V_{cmax}, J_{max}, and T_p) were investigated based on leaf gas-exchange measurements. Two experiments were conducted. In the first experiment (hereafter called Experiment 1), leaf gas-exchange measurements were repeated on the same leaves at four different times of day (08:30, 11:00, 13:30, and 16:00 h). In the second experiment (hereafter called Experiment 2), in contrast, leaves were randomly selected at each of the four diurnal measurements at 08:30, 11:00, 13:30, and 16:00 h. Experiment 1 was designed to investigate only the diurnal variations in the photosynthetic parameters without the inherent variations between leaves, whereas Experiment 2 was supplemental to Experiment 1 to ensure that the results obtained in Experiment 1 were not caused by order effects (*i.e.*, the influence of earlier measurements on later experiments); in Experiment 1, earlier gas-exchange measurements could damage the leaves and influence the later measurements, as the same leaves were repeatedly investigated within a day.

In both Experiment 1 and Experiment 2, healthy, fully expanded leaves were selected from the uppermost layers of the eggplant canopy, and the relationship between P_N and C_i (P_N–C_i curves) was obtained using two portable photosynthesis systems (*LI-6800*, *LI-COR Biosciences Inc.*, Nebraska, USA). After the leaves were clamped in a 2-cm^2 leaf chamber (*6800-01A*) and accustomed to saturating PPFD (1,200 µmol m^{-2} s^{-1}) for 8 min, the values of P_N and C_i were recorded at ambient CO_2 concentrations (C_a) of 400, 250, 100, 50, 400, 550, 700, 900; 1,200; and 1,500 µmol mol^{-1} in 1.5- to 2-min intervals (Long and Bernacchi 2003). At each CO_2 step, chlorophyll fluorescence measurements were conducted to estimate the quantum yield of PSII (Φ_{PSII}):

$$\Phi_{PSII} = (F_m' - F_s)/F_m' \tag{7}$$

where F_s is the steady-state fluorescence yield and F_m' is the light-adapted maximum fluorescence (Genty *et al.* 1989, Maxwell and Johnson 2000). F_s was measured at the end of each CO_2 step, and then a saturating light pulse [8,000 µmol(photon) m^{-2} s^{-1}] was applied to measure F_m'. From the measured Φ_{PSII}, the electron transport rate estimated from chlorophyll fluorescence (J_F) was obtained as $J_F = I\alpha_L\beta_{PSII}\Phi_{PSII}$, assuming $\alpha_L = 0.84$ and $\beta_{PSII} = 0.5$. A decline in J_F at high C_i is an indicator of TPU limitation (McClain and Sharkey 2019). During the measurements, the other environmental elements were set as follows: T_L = 25°C and RH = 60%. In Experiment 1, during the intervals between the four diurnal measurements at 08:30, 11:00, 13:30, and 16:00 h, the *LI-6800* leaf chambers were detached from the measured leaves until the next diurnal gas-exchange measurement. Additionally, in Experiment 1, each of the four diurnal gas-exchange measurements at 08:30, 11:00, 13:30, and 16:00 h was conducted using different positions of a leaf to reduce the effect of the previous measurements. Experiment 1 was conducted on 6, 7, 8, 13, and 14 April 2022, whereas Experiment 2 was conducted on 20, 21, and 22 April and 11 and 12 May. On each measurement day, different leaves were selected in both experiments. The sunrise and sunset times were approximately 05:30 and 18:30 h, respectively. Major environmental elements inside the greenhouse, including the air temperature ($T_{a,house}$), relative humidity (RH_{house}), CO_2 concentration ($C_{a,house}$), and outside solar radiation (S_{out}) were measured using a sensor unit (*House NAVI ADVANCE*, *Nippo*, Saitama, Japan). The water vapor pressure deficit (VPD_{house}) inside the greenhouse was calculated from $T_{a,house}$ and RH_{house}.

Parameter estimation: The measured P_N–C_i relationships were fit by the equations of the FvCB model (Eqs. 2, 3, and 4) to estimate the unknown parameters V_{cmax}, J_{max}, and T_p. Before curve fitting, fluorescence data (*i.e.*, J_F–C_i curves) simultaneously measured with P_N were used to determine which of the three photosynthetic limitations governs P_N; a J_F–C_i curve was separated into three sections showing increasing, constant, and declining J_F with an increase in C_i, and these sections were assigned with the limitations by Rubisco, RuBP-regeneration, and TPU, respectively (Long and Bernacchi 2003, McClain and Sharkey 2019). After visual inspection of the J_F–C_i curves, the region with C_i < 250 was assumed to be Rubisco limited (Eq. 2), and the region with $250 \leq C_i < 500$ was assumed to be RuBP-regeneration limited (Eq. 3), while the region with $500 \leq C_i$ was assumed to be TPU-limited (Eq. 4). Each of the three sections in the P_N–C_i curves was fit with the corresponding equation based on the Levenberg–Marquardt method using the *Python* '*lmfit*' package (*version 1.0.1*; Newville *et al.* 2014). For Rubisco-limited photosynthesis, two parameters, namely, V_{cmax} and R_d, were estimated by fitting Eq. 2. For RuBP-regeneration-limited photosynthesis, J was estimated by fitting Eq. 3 and then used to invert J_{max} from Eqs. 5 and 6. For TPU-limited photosynthesis, T_p and α were estimated by fitting Eq. 4. In the curve fitting processes for RuBP-regeneration-limited and TPU-limited photosynthesis, the R_d value was estimated in the Rubisco-limited curve fitting and used as a fixed parameter (Long and Bernacchi 2003). The values of the other parameters (*i.e.*, K_c, K_o, Γ^*, α_L, β_{PSII}, θ, and Φ_{max}) were obtained from the literature (Table 1). K_c, K_o, and Γ^* are thought to be intrinsic properties of the Rubisco enzyme and are commonly considered to be constant among terrestrial C_3 species to use the FvCB photosynthesis model (Medlyn *et al.* 2002, Long and Bernacchi 2003). Similarly, fixed values are often assigned to parameters related to photosynthetic light response (*i.e.*, α_L, β_{PSII}, θ, and Φ_{max}) for estimating J_{max} (von Caemmerer 2000).

Statistical analysis: The effect of time of day on each of the three parameters (*i.e.*, V_{cmax}, J_{max}, and T_p) was statistically evaluated. The values of each parameter were grouped according to the four measurement timings (*i.e.*, 8:30, 11:00, 13:30, and 16:00 h), and an overall difference among the four groups was determined by analysis of variance (*ANOVA*). In Experiment 1, one-way repeated-measures *ANOVA* was applied because the same samples (*i.e.*, leaves) were repeatedly measured at each time point, whereas in Experiment 2, one-way *ANOVA* was applied because the samples were independently measured at each time point. Before these *ANOVA*s, necessary assumptions were tested; for the one-way repeated-measures *ANOVA* in Experiment 1, normality and sphericity were tested with a *Shapiro–Wilk* test and *Mauchly*'s test, respectively, and for the one-way *ANOVA* in Experiment 2, normality and homogeneity of variances were tested with a *Shapiro–Wilk* test and *Bartlett*'s test. After the *ANOVA*s, differences between individual groups (*i.e.*, differences between the means of each parameter at 8:30, 11:00, 13:30, and 16:00 h) in both experiments were tested by the *Holm–Bonferroni* method.

The statistical analyses were performed using *scipy* (*1.7.3*), *statsmodels* (*0.13.2*), and *pingouin* (*0.5.1*), free software libraries available in *Python* (the numbers in parentheses indicate the software versions).

Results

Micrometeorology: The environmental conditions inside the greenhouse were different every measurement day. The daily integrals of S_{out} ranged between 10.7 and 23.5 MJ m^{-2} in Experiment 1 and between 3.5 and

Table 1. Parameter values for estimating the maximal carboxylation rate (V_{cmax}), the maximal electron transport rate (J_{max}), and the rate of triose phosphate export from the chloroplast (T_p).

Symbol	Description	Value	Source
K_c	Michaelis–Menten constants of Rubisco for carboxylation [μmol mol^{-1})]	404.9	Bernacchi *et al.* (2001)
K_o	Michaelis–Menten constants of Rubisco for oxygenation [mmol mol^{-1}]	278.4	Bernacchi *et al.* (2001)
Γ^*	CO_2-compensation point without R_d [μmol mol^{-1}]	42.75	Bernacchi *et al.* (2001)
α_L	Absorptance of leaves [–]	0.84	von Caemmerer (2000)
β_{PSII}	Fraction of absorbed PPFD that reaches photosystem II [–]	0.5	von Caemmerer (2000)
θ	Empirical curvature factor [–]	0.7	von Caemmerer (2000)
Φ_{max}	The maximum quantum yield of photosystem II [–]	0.85	von Caemmerer (2000)

24.3 MJ m^{-2} in Experiment 2. The means of $T_{a,house}$ between 08:30 and 16:00 h were relatively stable and ranged between 23.9 and 26.0°C in Experiment 1 and between 21.0 and 25.4°C in Experiment 2. The daily means of $C_{a,house}$ were similar on every measurement day and were 411 ± 5 in Experiment 1 and 435 ± 21 µmol mol^{-1} in Experiment 2 (the values after the ± signs indicate the standard deviations). The daily means of VPD_{house} ranged between 2.0 and 2.5 kPa in Experiment 1 and between 2.2 and 2.6 kPa in Experiment 2.

The environmental conditions (*i.e.*, the daily integral of S_{out} and the daytime means of $T_{a,house}$, $C_{a,house}$, and VPD_{house}) on the measurement days had no significant effects on diurnal changes in V_{cmax}, J_{max}, and T_p; there were no significant correlations between any combinations of the environmental variables and diurnal changes in the photosynthetic parameters from 08:30 to 16:00 h (the *p* values of the *Pearson*'s correlation coefficients were > 0.05) in either Experiment 1 or Experiment 2.

P_N–C_i and J_F–C_i curves: Fig. 1*A,C* shows the P_N–C_i curves measured at four different times of day (08:30, 11:00, 13:30, and 16:00 h). In both Experiment 1 and 2, P_N showed a typical response to C_i; with increasing C_i, P_N increased rapidly at low C_i and then saturated quickly at a C_i value of approximately 500 µmol mol^{-1}. However, the saturation values of P_N differed depending on the times of day at which the P_N–C_i curves were obtained; P_N–C_i curves were the highest at 08:30 h and gradually decreased as the time advanced. In both Experiment 1 and Experiment 2, differences between the P_N–C_i curves appeared smaller at low C_i values (< 250 µmol mol^{-1}) than those at higher C_i values.

Fig. 1*B,D* shows the J_F–C_i curves measured simultaneously with the P_N–C_i curves. In contrast to the P_N–C_i curves, the J_F–C_i curves did not show saturating responses to increasing C_i; rather, J_F showed a gradual decline with increasing C_i above approximately 500 µmol mol^{-1}. A decrease in J_F with increasing C_i is indicative of the TPU limitation of photosynthesis (McClain and Sharkey 2019); when TPU limits photosynthesis, an increase in C_i allows Rubisco to bind more readily with CO_2 and less with O_2, but this increase in Rubisco-CO_2 binding does not lead to an increase in the carboxylation of RuBP due to the limited availability of inorganic phosphate in the chloroplast. Additionally, the deficiency of inorganic phosphate is exacerbated by reductions in Rubisco-O_2 binding and RuBP oxygenation, through which inorganic phosphate can be produced. Consequently, Rubisco activity and electron transport are slowed to match the availability of inorganic phosphate, leading to a reduction in J_F with increasing C_i.

V_{cmax}, J_{max}, and T_p: Fig. 2 shows the diurnal variations in the three parameters representing photosynthetic capacity. Overall, all three parameters tended to decline as the time of day advanced, and significant effects of time of day on all three parameters were found in both Experiment 1 and Experiment 2. In Experiment 1, the *p* values calculated by one-way repeated-measures *ANOVA* were 0.012, 0.017, and < 0.01 for V_{cmax}, J_{max}, and T_p, respectively. Similarly, in Experiment 2, the *p* values calculated by one-way *ANOVA* were < 0.01 for all three parameters (V_{cmax}, J_{max}, and T_p). The necessary assumptions for applying *ANOVA*s (*i.e.*, normality and sphericity for Experiment 1 and normality and equal variances for Experiment 2) were not violated in either Experiment 1 or Experiment 2 (p>0.05). Thus, these results strongly suggest that measurement time influences the values of V_{cmax}, J_{max}, and T_p.

In Experiment 1, V_{cmax} and J_{max} remained relatively stable until 13:30 h but declined considerably at 16:00 h; the mean values of both V_{cmax} and J_{max} declined by 15% at 16:00 h compared to those at 08:30 h. However, the *Holm–Bonferroni* multiple comparison test failed to detect a significant difference between parameters measured at different times of day at the 5% level of significance.

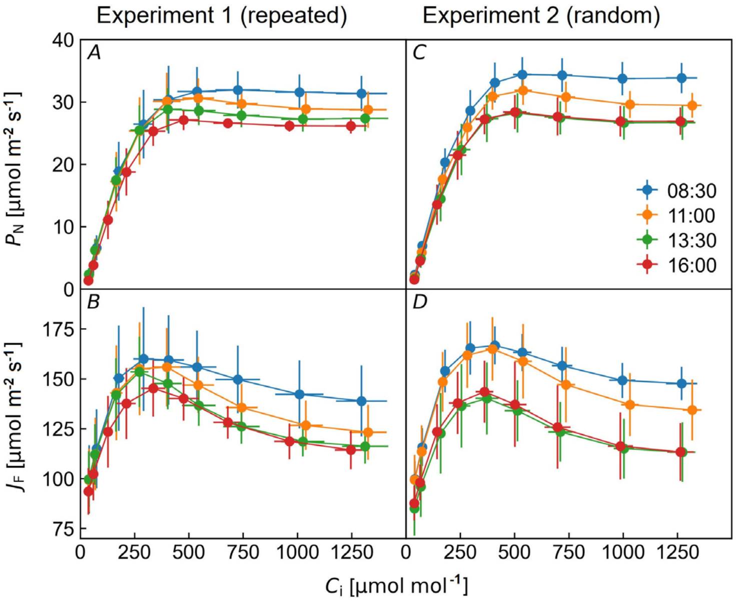

Fig. 1. Responses of the (*A*,*C*) single-leaf photosynthetic rate (P_N) and (*B*,*D*) electron transport rate (J_F) to varying intercellular CO_2 concentrations (C_i) measured at four different times of the day (08:30, 11:00, 13:30, and 16:00 h). The results of both Experiment 1 and Experiment 2 are shown. In Experiment 1, measurements were repeated on the same leaves at four different times of day, whereas in Experiment 2, leaves were randomly selected for each of the four diurnal measurements. The points and error bars indicate the means and standard deviations, respectively (n = 9).

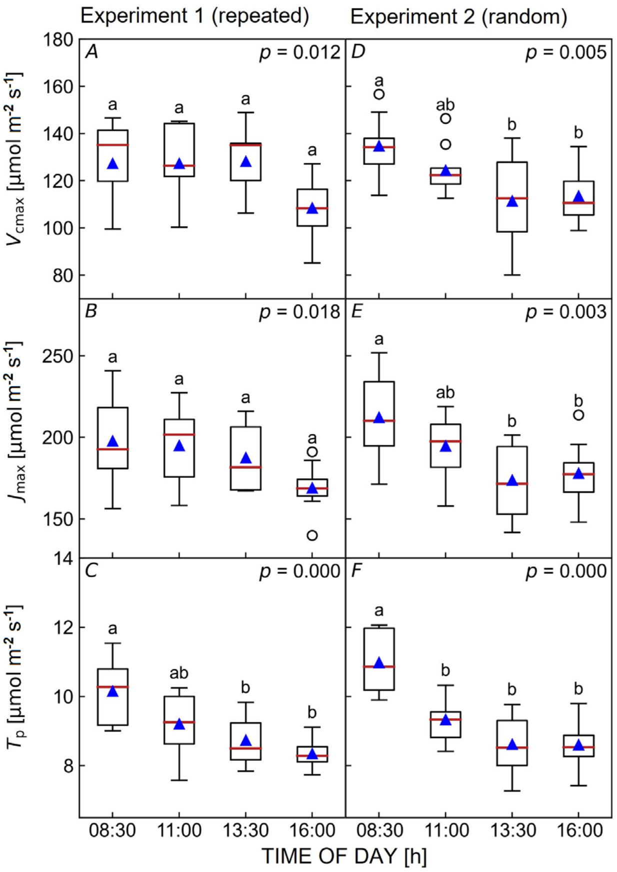

Fig. 2. Diurnal variations in the (*A*,*D*) maximal carboxylation rate (V_{cmax}), (*B*,*E*) maximal electron transport rate (J_{max}), and (*C*,*F*) triose phosphate-utilization rate (T_{p}). These parameters were estimated from P_{N}–C_{i} curves measured at four different times of day (08:30, 11:00, 13:30, and 16:00 h). Each of the boxes represents the middle 50% of the data, and *the red line* in each box indicates the median. The whiskers on the box plots extend to the most extreme data points except for outliers (*i.e.*, values whose distance from the top/bottom of a box exceeds 1.5 times the box height), which are represented by *circles*. *The blue triangles* indicate the means. Means with *a common letter* are not significantly different by the *Holm–Bonferroni* method at the 5% level of significance. The *p* values shown in the figures were calculated using one-way repeated-measures *ANOVA* in Experiment 1 and one-way *ANOVA* in Experiment 2.

In contrast, T_{p} showed a gradual decline over time. The percentage decline in T_{p} from 08:30 to 16:00 h was more considerable (18%) than those of V_{cmax} and J_{max}. As a result, the *Holm–Bonferroni* multiple comparison test indicated that the T_{p} measured at 08:30 h was significantly different from those measured in the afternoon (*i.e.*, 13:30 and 16:00 h).

In Experiment 2, the means of V_{cmax}, J_{max}, and T_{p} were the highest at 08:30 h and decreased at 11:30 h. They further declined at 13:30 h and remained relatively stable until 16:00 h. The *Holm–Bonferroni* multiple comparison test determined that V_{cmax} and J_{max} measured at 08:30 h were significantly different from those measured in the afternoon (*i.e.*, 13:30 and 16:00 h). Additionally, the T_{p} measured at 08:30 h was significantly different from those measured at the other times of the day. The percentage declines in V_{cmax}, J_{max}, and T_{p} from 08:30 to 16:00 h were 16, 16, and 22%, respectively.

Discussion

The results of both Experiment 1 and Experiment 2 indicate that the V_{cmax}, J_{max}, and T_{p} of the uppermost leaves in an eggplant canopy can vary diurnally and tend to be higher in the morning than in the afternoon. The observed changes in the P_{N}–C_{i} curves and J_{F}–C_{i} were similar to the results reported by Fabre *et al.* (2019), in which P_{N}–C_{i} curves and Φ_{PSII}–C_{i} curves (note that J_{F} and Φ_{PSII} are proportional) were obtained using panicle-pruned rice under elevated CO_2 treatment. The authors reported that T_{p} is linearly related to the concentration of leaf sucrose and suggested that increased accumulation of nonstructural carbohydrates in leaves is involved in the regulation of photosynthesis. Although the present study did not impose any severe sink restriction (*i.e.*, fruit pruning), it is likely that leaf nonstructural carbohydrates progressively accumulated toward the end of the day, as recently reported in greenhouse-grown strawberries (Nakai *et al.* 2022).

Other biological mechanisms that may explain the diurnal decline in V_{cmax}, J_{max}, and T_{p} are changes in mesophyll conductance (Flexas *et al.* 2013). Mesophyll conductance determines the supply of CO_2 from the intercellular airspace to the chloroplast and can change diurnally in response to environmental conditions (Flexas *et al.* 2013) and times of the day (Nascimento and Marenco 2013). A decline in mesophyll conductance can reduce the supply of CO_2 to the chloroplast and decrease apparent V_{cmax} and J_{max} calculated based on C_{i} (intercellular CO_2 concentration) rather than chloroplast CO_2 concentration (Flexas *et al.* 2008). A decline in mesophyll conductance in the afternoon was reported for Amazonian saplings in the understory (Nascimento and Marenco 2013), although its cause was not fully identified (endogenous factors such as a biological clock were suggested). A similar diurnal decline in mesophyll conductance may have occurred in the uppermost leaves of the eggplant canopy.

Some of the abovementioned possible causes of declines in photosynthetic parameters may be interrelated; the accumulation of nonstructural carbon, which is associated with a decline in T_{p}, can cause the movement of chloroplasts to reduce their surface area adjacent to intercellular airspaces (Tholen *et al.* 2008, Maai *et al.* 2020). This can cause a decline in the mesophyll conductance, leading to a decline in apparent V_{cmax} and J_{max} calculated based on C_{i}.

The results of the present study suggest that care must be taken when interpreting the values of V_{cmax}, J_{max}, and T_{p} obtained at different times of day; V_{cmax}, J_{max}, and T_{p} can vary by as much as 22% during the day. This value is within the range reported in the literature on diurnal variations in photosynthetic capacity (Singsaas *et al.* 2000, Kets *et al.* 2010, Fabre *et al.* 2019, Stinziano *et al.* 2020);

for example, Stinziano *et al.* (2020) reported a decline in V_{cmax} as great as 50% in several species, while Nascimento and Marenco (2013) reported no significant difference in the V_{cmax} of two Amazonian saplings measured in the morning, midday, and afternoon. Since obtaining one P_N–C_i curve requires *ca*. 30 min, it may be recommended to apply faster techniques such as the rapid P_N–C_i response (RACiR) technique (Stinziano *et al.* 2017, 2020) and one-point method (De Kauwe *et al.* 2016) to obtain many samples of V_{cmax}, J_{max}, and T_p within a limited duration. Additionally, when estimating P_N by the FvCB model, the use of V_{cmax}, J_{max}, and T_p estimated from morning measurements may result in the overestimation of P_N.

References

Baldocchi D.D.: Assessing the eddy covariance technique for evaluating carbon dioxide exchange rates of ecosystems: past, present and future. – Glob. Change Biol. **9**: 479-492, 2003.

Ball J.T., Woodrow I.E., Berry J.A.: A model predicting stomatal conductance and its contribution to the control of photosynthesis under different environmental conditions. – In: Biggins J. (ed.): Progress in Photosynthesis Research. Pp. 221-224. Springer, Dordrecht 1987.

Bernacchi C.J., Pimentel C., Long S.P.: *In vivo* temperature response functions of parameters required to model RuBP-limited photosynthesis. – Plant Cell Environ. **26**: 1419-1430, 2003.

Bernacchi C.J., Singsaas E.L., Pimentel C. *et al.*: Improved temperature response functions for models of Rubisco-limited photosynthesis. – Plant Cell Environ. **24**: 253-259, 2001.

Brodribb T.J., Holbrook N.M.: Diurnal depression of leaf hydraulic conductance in a tropical tree species. – Plant Cell Environ. **27**: 820-827, 2004.

Collatz G.J., Ball J.T., Grivet C., Berry J.A.: Physiological and environmental regulation of stomatal conductance, photosynthesis and transpiration: a model that includes a laminar boundary layer. – Agr. Forest Meteorol. **54**: 107-136, 1991.

De Kauwe M.G., Lin Y.S., Wright I.J. *et al.*: A test of the 'one-point method' for estimating maximum carboxylation capacity from field-measured, light-saturated photosynthesis. – New Phytol. **210**: 1130-1144, 2016.

De Pury D.G.G., Farquhar G.D.: Simple scaling of photosynthesis from leaves to canopies without the errors of big-leaf models. – Plant Cell Environ. **20**: 537-557, 1997.

Fabre D., Yin X., Dingkuhn M. *et al.*: Is triose phosphate utilization involved in the feedback inhibition of photosynthesis in rice under conditions of sink limitation? – J. Exp. Bot. **70**: 5773-5785, 2019.

Farquhar G.D., von Caemmerer S., Berry J.A.: A biochemical model of photosynthetic CO_2 assimilation in leaves of C_3 species. – Planta **149**: 78-90, 1980.

Flexas J., Ribas-Carbó M., Diaz-Espejo A. *et al.*: Mesophyll conductance to CO_2: Current knowledge and future prospects. – Plant Cell Environ. **31**: 602-621, 2008.

Flexas J., Scoffoni C., Gago J., Sack L.: Leaf mesophyll conductance and leaf hydraulic conductance: An introduction to their measurement and coordination. – J. Exp. Bot. **64**: 3965-3981, 2013.

Gaastra P.: Photosynthesis of crop plants as influenced by light, carbon dioxide, temperature, and stomatal diffusion resistance. PhD Thesis. Pp. 68. Wageningen University 1959.

Genty B., Briantais J.M., Baker N.R.: The relationship between the quantum yield of photosynthetic electron transport and quenching of chlorophyll fluorescence. – BBA-Gen. Subjects **990**: 87-92, 1989.

Jones H.G.: Plants and Microclimate: A Quantitative Approach to Environmental Plant Physiology. Pp. 407. Cambridge University Press, Cambridge 2013.

Kets K., Darbah J.N.T., Sober A. *et al.*: Diurnal changes in photosynthetic parameters of *Populus tremuloides*, modulated by elevated concentrations of CO_2 and/or O_3 and daily climatic variation. – Environ. Pollut. **158**: 1000-1007, 2010.

Kimura K., Yasutake D., Koikawa K., Kitano M.: Spatiotemporal variability of leaf photosynthesis and its linkage with microclimates across an environment-controlled greenhouse. – Biosyst. Eng. **195**: 97-115, 2020.

Larkum A.W.D.: Limitations and prospects of natural photosynthesis for bioenergy production. – Curr. Opin. Biotech. **21**: 271-276, 2010.

Leakey A.D.B., Ainsworth E.A., Bernacchi C.J. *et al.*: Elevated CO_2 effects on plant carbon, nitrogen, and water relations: Six important lessons from FACE. – J. Exp. Bot. **60**: 2859-2876, 2009.

Long S.P., Bernacchi C.J.: Gas exchange measurements, what can they tell us about the underlying limitations to photosynthesis? Procedures and sources of error. – J. Exp. Bot. **54**: 2393-2401, 2003.

Maai E., Nishimura K., Takisawa R., Nakazaki T.: Light stress-induced chloroplast movement and midday depression of photosynthesis in sorghum leaves. – Plant Prod. Sci. **23**: 172-181, 2020.

Maxwell K., Johnson G.N.: Chlorophyll fluorescence – a practical guide. – J. Exp. Bot. **51**: 659-668, 2000.

McClain A.M., Sharkey T.D.: Triose phosphate utilization and beyond: From photosynthesis to end product synthesis. – J. Exp. Bot. **70**: 1755-1766, 2019.

Medlyn B.E., Dreyer E., Ellsworth D. *et al.*: Temperature response of parameters of a biochemically based model of photosynthesis. II. A review of experimental data. – Plant Cell Environ. **25**: 1167-1179, 2002.

Medlyn B.E., Duursma R.A., Eamus D. *et al.*: Reconciling the optimal and empirical approaches to modelling stomatal conductance. – Glob. Change Biol. **17**: 2134-2144, 2011.

Murchie E.H., Lawson T.: Chlorophyll fluorescence analysis: A guide to good practice and understanding some new applications. – J. Exp. Bot. **64**: 3983-3998, 2013.

Nakai H., Yasutake D., Kimura K. *et al.*: Dynamics of carbon export from leaves as translocation affected by the coordination of carbohydrate availability in field strawberry. – Environ. Exp. Bot. **196**: 104806, 2022.

Nascimento H.C.S., Marenco R.A.: Mesophyll conductance variations in response to diurnal environmental factors in *Myrcia paivae* and *Minquartia guianensis* in Central Amazonia. – Photosynthetica **51**: 457-464, 2013.

Newville M., Stensitzki T., Allen D.B. *et al.*: LMFIT: Non-linear least-square minimization and curve-fitting for Python, 2014. *Available at*: https://lmfit.github.io/lmfit-py/.

Nomura K., Yasutake D., Kaneko T. *et al.*: Long-term estimation of the canopy photosynthesis of a leafy vegetable based on greenhouse climate conditions and nadir photographs. – Sci. Hortic.-Amsterdam **289**: 110433, 2021.

Parelle J., Roudaut J.-P., Ducrey M.: Light acclimation and photosynthetic response of beech (*Fagus sylvatica* L.) saplings under artificial shading or natural Mediterranean conditions. – Ann. For. Sci. **63**: 257-266, 2006.

Piao S., Sitch S., Ciais P. *et al.*: Evaluation of terrestrial carbon cycle models for their response to climate variability and to CO_2 trends. – Glob. Change Biol. **19**: 2117-2132, 2013.

Prior S.A., Runion G.B., Marble S.C. *et al.*: A review of elevated atmospheric CO_2 effects on plant growth and water relations: Implications for horticulture. – HortScience **46**: 158-162, 2011.

Rogers A., Medlyn B.E., Dukes J.S. *et al.*: A roadmap for improving the representation of photosynthesis in Earth system models. – New Phytol. **213**: 22-42, 2017.

Ryu Y., Berry J.A., Baldocchi D.D.: What is global photosynthesis? History, uncertainties and opportunities. – Remote Sens. Environ. **223**: 95-114, 2019.

Sharkey T.D.: Photosynthesis in intact leaves of C_3 plants: Physics, physiology and rate limitations. – Bot. Rev. **51**: 53-105, 1985.

Singsaas E.L., Ort D.R., DeLucia E.H. *et al.*: Diurnal regulation of photosynthesis in understory saplings. – New Phytol. **145**: 39-49, 2000.

Stinziano J., Harjoe M., Roback C. *et al.*: Photosynthetic capacity exhibits diurnal variation, implications for terrestrial biosphere models and gas exchange measurements. – Authorea, 1-25, 2020.

Stinziano J.R., Morgan P.B., Lynch D.J. *et al.*: The rapid A-C_i response: photosynthesis in the phenomic era. – Plant Cell Environ. **40**: 1256-1262, 2017.

Tanizaki T., Yokoyama G., Kitano M., Yasutake D.: Contribution of diffusional and non-diffusional limitations to the midday depression of photosynthesis which varies dynamically even under constant environmental conditions. – Int. Agrophys. **36**: 207-212, 2022.

Tholen D., Boom C., Noguchi K. *et al.*: The chloroplast avoidance response decreases internal conductance to CO_2 diffusion in *Arabidopsis thaliana* leaves. – Plant Cell Environ. **31**: 1688-1700, 2008.

von Caemmerer S.: Biochemical Models of Leaf Photosynthesis. Pp. 165. CSIRO Publishing, Collingwood 2000.

Walker A.P., Quaife T., van Bodegom P.M. *et al.*: The impact of alternative trait-scaling hypotheses for the maximum photosynthetic carboxylation rate (V_{cmax}) on global gross primary production. – New Phytol. **215**: 1370-1386, 2017.

Yamori W., Hikosaka K., Way D.A.: Temperature response of photosynthesis in C_3, C_4, and CAM plants: Temperature acclimation and temperature adaptation. – Photosynth. Res. **119**: 101-117, 2014.